
JOURNAL OF THE AMERICAN CHEMICAL SOCIETY

Direct Observation of Hydrogen Bonds in Nucleic Acid Base Pairs by Internucleotide $^2J_{\text{NN}}$ Couplings

Andrew J. Dingley[†] and Stephan Grzesiek^{*,†,‡}

Contribution from the Institute of Physical Biology, Heinrich-Heine-Universität, 40225 Düsseldorf, Germany, and Institute of Structural Biology, IBI-2, Forschungszentrum Jülich, 52425 Jülich, Germany

Received May 1, 1998

Abstract: Hydrogen bonds play a key role in the stabilization of protein and nucleic acid secondary structure. Currently, most of the experimental evidence for the interaction of hydrogen bond donor and acceptor atoms is indirect. Here we show that scalar couplings across the hydrogen bond are observable for Watson–Crick base pairs in ^{15}N -labeled RNA. These scalar couplings correlate the imino donor ^{15}N nucleus and the corresponding acceptor ^{15}N nucleus on the complementary base. The two-bond J_{NN} couplings between the N3 of uridine and the N1 of adenosine, and between the N1 of guanosine and the N3 of cytidine, have values of approximately 7 Hz as determined by a novel quantitative J -correlation experiment for the 69-nucleotide T1 domain of the potato spindle tuber viroid. In contrast, for non-Watson–Crick base pairs the hydrogen bond acceptor is usually not a nitrogen, but an oxygen atom, and thus, the two-bond J_{NN} couplings are not observed.

Hydrogen bonds play a key role in the stabilization of protein and nucleic acid secondary structure and in modulating the speed and specificity of enzymatic reactions.^{1–3} Very few experimental parameters exist that provide direct evidence of individual hydrogen bonds, and thus, identify all atoms involved in the hydrogen bond, i.e., the donor atom, the acceptor atom, as well as the hydrogen atom itself. Usually the existence of hydrogen bonds is inferred a posteriori from the spatial proximity and relative orientation of the hydrogen bond donor, the hydrogen, and the hydrogen bond acceptor once the structure of a biomolecule has been solved by either X-ray crystallography or NMR. A number of NMR observables provide indirect

evidence for individual hydrogen bonds. Such parameters include the following: (i) the reduced hydrogen exchange rates with the solvent;^{4,5} (ii) the primary isotope shifts for substitution of the hydrogen bonded proton by ^2H and ^3H ;^{6,7} (iii) the isotropic proton chemical shift;⁸ (iv) the isotropic nitrogen chemical shift;⁹ (v) the size of the electric field gradient at the position of the proton as observed by the ^2H quadrupolar coupling constant;^{10,11} and (vi) the size of the proton chemical shift anisotropy.^{12,13}

* Address correspondence to this author at the Forschungszentrum Jülich.
[†] Heinrich-Heine-Universität.

[‡] Forschungszentrum Jülich.

(1) Jeffrey, G. A.; Saenger, W. *Hydrogen Bonding in Biological Structures*; Springer-Verlag: New York, 1991.

(2) Saenger, W. *Principles of Nucleic Acid Structure*; Cantor, C. R., Series Ed.; Springer-Verlag: New York, 1984.

(3) Fersht, A. *Enzyme Structure and Mechanism*, 2nd Ed.; W. H. Freeman: New York, 1985.

(4) Hvidt, A.; Nielsen, S. O. *Adv. Protein Chem.* **1966**, *21*, 287–386.

(5) Wagner, G. *Q. Rev. Biophys.* **1983**, *16*, 1–57.

(6) Gunnarsson, G.; Wennerström, H.; Ega, W.; Forsen, S. *Chem. Phys. Lett.* **1976**, *38*, 96–99.

(7) Altman, L. J.; Laungani, D.; Gunnarsson, G.; Wennerström, H.; Forsen, S. *J. Am. Chem. Soc.* **1978**, *100*, 8264–8266.

(8) Shoup, R. R.; Miles, H. T.; Becker, E. D. *Biochem. Biophys. Res. Commun.* **1966**, *23*, 194–201.

(9) Markowski, V.; Sullivan, G. R.; Roberts, J. D. *J. Am. Chem. Soc.* **1977**, *99*, 714–718.

(10) Boyd, J.; Mal, T. K.; Soffe, N.; Campbell, I. D. *J. Magn. Reson.* **1997**, *124*, 61–71.

(11) LiWang, A. C.; Bax, A. *J. Magn. Reson.* **1997**, *127*, 54–64.

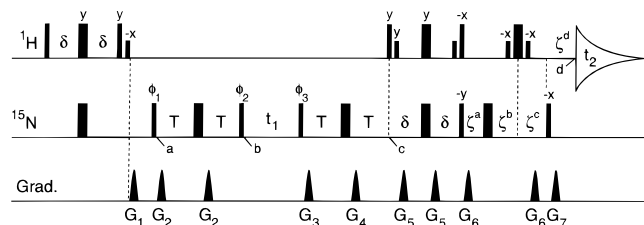


Figure 1. Pulse sequence of the quantitative J_{NN} HNN-COSY experiment. Narrow and wide pulses correspond to flip angles of 90° and 180° , respectively. RF power levels for high-power pulses are 29 (^1H) and 5.8 kHz (^{15}N). Low-power ^1H pulses are applied at a field strength of 200 Hz. Carrier positions are $^1\text{H}_2\text{O}$ (^1H), 185 ppm (^{15}N), and 153 ppm (^{13}C). Garp decoupling ($\gamma B_2 = 2.5$ kHz) was applied during the t_1 period on the ^{13}C channel. Delays: $\delta = 2.25$ ms; $T = 15$ ms; $\zeta^a = 2.5$ ms; $\zeta^b = 0.25$ ms; $\zeta^c = 2.25$ ms; $\zeta^d = 0.5$ ms. Unless indicated, all pulses are applied along the x axis. Phase cycling: $\phi_1 = x, y, -x, -y$; $\phi_2 = R_2, -R_2$ with $R_2 = (y, -x, -y, x)$; $\phi_3 = R_3, R_3, -R_3, -R_3$ with $R_3 = (-y, x, y, -x)$; Acq. = $x, -y, -x, y$. Quadrature detection in the t_1 dimension was achieved by simultaneously incrementing ϕ_1 and ϕ_2 in the States-TPPI manner. Gradients are sine-bell shaped, with an absolute amplitude of 25 G/cm at their center and durations (polarities) of $G_{1,2,3,4,5,6,7} = 2.5$ (+), 2.1 (−), 1.35 (+), 2.35 (+), 0.2 (+), 0.4 (+), and 0.101 ms (+).

Here we report the direct observation of hydrogen bonding in Watson–Crick base pairs by a cross hydrogen bond scalar coupling between the imino ^{15}N atom of the donor base with the hydrogen bond acceptor ^{15}N atom on the complementary base. These $^2J_{NN}$ couplings yield valuable through-bond inter-residue assignment information.

Experimental Section

NMR experiments were performed on a uniformly $^{13}\text{C}/^{15}\text{N}$ -enriched 69 nucleotide RNA oligomer (GGGUGUGUAG CCCUUGGAAC CGCAGUUGGU UCCUCGGAAC UAAACUCGUG GUUCCUGUGG UUCACACCC). This oligomer comprises the left terminal (T1) domain of the potato spindle tuber viroid¹⁴ (PSTVd). A 250 μL sample volume was used in a Shigemi microcell containing 1.6 mM RNA oligomer, 100 mM NaCl, 10 mM $\text{NaH}_2\text{PO}_4/\text{Na}_2\text{HPO}_4$, and 95% $\text{H}_2\text{O}/5\%$ D_2O at pH 6.0. All NMR data were acquired at 25 $^\circ\text{C}$ on a Bruker DMX-600 NMR spectrometer equipped with a triple-axis pulsed field gradient $^1\text{H}/^{15}\text{N}/^{13}\text{C}$ probehead optimized for ^1H detection.

The quantitative J_{NN} HNN-COSY experiment depicted in Figure 1 was used to measure homonuclear ^{15}N – ^{15}N J coupling constants on the PSTVd T1 domain. The data matrix consisted of $250^*(t_1) \times 1024^*(t_2)$ data points (where n^* refers to complex points) with acquisition times of 40 (t_1) and 77 ms (t_2). A total of 128 scans per complex t_1 increment was collected.

The $^2J_{HN}$ HSQC experiment was recorded as a conventional WATERGATE,¹⁵ water flip-back¹⁶ ^1H – ^{15}N HSQC with the INEPT transfer delays set to 11 ms as a compromise between the fast relaxation of the $^1\text{H}_2$ resonance and the optimal transfer time for the two-bond $^1\text{H}_2$ – $^{15}\text{N}_1$ and $^1\text{H}_2$ – $^{15}\text{N}_3$ couplings of 14.5 Hz.¹⁷ The data matrix consisted of $180^*(t_1) \times 1024^*(t_2)$ data points with acquisition times of 31 (t_1) and 77 ms (t_2). A total of 192 scans per complex t_1 increment was collected. The total measuring time was 13.2 h. The experiment was performed with the ^1H carrier positioned on the H_2O resonance,

the ^{15}N carrier at 215 ppm, and the ^{13}C carrier at 154 ppm. Simultaneous ^{15}N and ^{13}C decoupling was applied during data acquisition.

A 3D NOESY was recorded as a $^1\text{H}_C(t_1)$ –HMQC– $^{13}\text{C}(t_2)$ –NOE– $^1\text{H}(t_3)$ experiment with optimized detection of imino-proton resonances by water flip-back,¹⁶ WATERGATE,¹⁵ and radiation damping¹⁸ techniques. The data matrix consisted of $46^*(t_1) \times 48^*(t_2) \times 1024^*(t_3)$ data points with acquisition times of 7 (t_1), 12 (t_2), and 68 ms (t_3), and an NOE mixing time of 80 ms. The total experimental time was 60 h. The ^1H carrier was positioned on the H_2O resonance, the ^{13}C carrier at 110 ppm, and the ^{15}N carrier at 153 ppm. ^{15}N decoupling was applied during data acquisition.

Data sets were processed using the program nmrPipe,¹⁹ and peak positions determined with the program PIPP.²⁰ Amplitudes of the time domain oscillations in the quantitative J_{NN} HNN-COSY data set were determined by using the time domain fitting routine nlinLS contained in the NMRPipe¹⁹ package.

Results and Discussion

Homonuclear J_{NN} couplings involving the imino ^{15}N nuclei in RNA were observed and quantified by using the quantitative J_{NN} correlation experiment depicted in Figure 1. The experiment is conceptually similar to the quantitative $^3J_{\text{HNHA}}$ COSY experiment.²¹ The following product operator description will be given for the uridine-adenosine (U-A) base pair (Figure 2A) where N3 of U is the donor nitrogen, H3 of U the hydrogen bond proton, and N1 of A the acceptor nitrogen. The analogous description for the guanosine-cytidine (G-C) base pair is obtained by interchanging the U-A nuclei H3, N3, and N1 with the G-C nuclei H1, N1, and N3 (Figure 2B). Magnetization is transferred from the imino proton of one base to its attached nitrogen nucleus at point *a* to give an operator product of the form $2\text{H}_3\text{z}_2\text{N}_3\text{y}$. Due to the observed scalar coupling between the hydrogen bond donor and acceptor nuclei, part of this magnetization is transferred onto the $^{15}\text{N}_1$ nucleus of the opposing adenosine during the interval $2T$. At point *b*, this magnetization is given as $-4\text{H}_3\text{z}_2\text{N}_3\text{z}_1\text{N}_1\text{y}\sin(2\pi J_{NN}T)$. Another part of the magnetization remains on the imino ^{15}N nucleus of the hydrogen donor base. The product operator for this part is proportional to $2\text{H}_3\text{z}_2\text{N}_3\text{y}\cos(2\pi J_{NN}T)$. During the variable delay t_1 , the oscillations of both transverse magnetization terms are measured leading to diagonal and cross-peaks in the f_1 dimension at the ^{15}N frequencies of the imino nitrogen N3 of uridine and the hydrogen bond acceptor nitrogen N1 on adenosine. Subsequently, both magnetization terms are refocused during the second $2T$ interval to give $2\text{H}_3\text{z}_2\text{N}_3\text{y}$ at position *c*. Therefore, intensities for cross and diagonal peaks are proportional to $\sin^2(2\pi J_{NN}T)$ and $\cos^2(2\pi J_{NN}T)$, respectively.

The description so far has neglected relaxation effects. Interference between dipole–dipole interaction and ^{15}N chemical shift anisotropy (CSA) interaction gives rise to two different relaxation rates, $R_2 + \eta$ and $R_2 - \eta$, for the two components $\text{H}_\alpha\text{N}_\text{y}$ and $\text{H}_\beta\text{N}_\text{y}$ of the ^{15}N – ^1H doublet.^{22–24} The nitrogen antiphase magnetization at time point *a* $2\text{H}_3\text{z}_2\text{N}_3\text{y}$ is identical to the operator difference $\text{H}_3\alpha\text{N}_3\text{y} - \text{H}_3\beta\text{N}_3\text{y}$. Due to the different relaxation rates of the two components, the magnetization at

(18) Lippens, G.; Dhalluin, C.; Wieruszski, J. M. *J. Biomol. NMR* **1995**, *5*, 327–331.

(19) Delaglio, F.; Grzesiek, S.; Vuister, G. W.; Zhu, G.; Pfeifer, J.; Bax, A. *J. Biomol. NMR* **1995**, *6*, 277–293.

(20) Garrett, D. S.; Powers, R.; Gronenborn, A. M.; Clore, G. M. *J. Magn. Reson.* **1991**, *95*, 214–220.

(21) Vuister, G. W.; Bax, A. *J. Am. Chem. Soc.* **1993**, *115*, 7772–7777.

(22) Goldman, M. *J. Magn. Reson.* **1984**, *60*, 437–452.

(23) Tjandra, N.; Szabo, A.; Bax, A. *J. Am. Chem. Soc.* **1996**, *118*, 6986–6991.

(24) Pervushin, K.; Riek, R.; Wider, G.; Wüthrich, K. *Proc. Natl. Acad. Sci. U.S.A.* **1997**, *94*, 12366–12371.

(12) Tjandra, N.; Bax, A. *J. Am. Chem. Soc.* **1997**, *119*, 8076–8082.

(13) Tessari, M.; Vis, H.; Boelens, R.; Kaptein, R.; Vuister, G. W. *J. Am. Chem. Soc.* **1997**, *119*, 8985–8990.

(14) Gross H. J.; Domdey, H.; Lossow, C.; Jank, P.; Raba, M.; Alberty, H.; Sanger, H. L. *Nature* **1978**, *273*, 203–208.

(15) Piotto, M.; Saudek, V.; Sklenar, V. *J. Biomol. NMR* **1992**, *2*, 661–665.

(16) Grzesiek, S.; Bax, A. *J. Am. Chem. Soc.* **1993**, *115*, 12593–12594.

(17) Ippel, J. H.; Wijmenga, S. S.; de Jong, R.; Heus, H. A.; Hilbers, C. W.; de Vroom, E.; van der Marcel, G. A.; van Boom, J. H. *Magn. Reson. Chem.* **1996**, *34*, S156–S176.

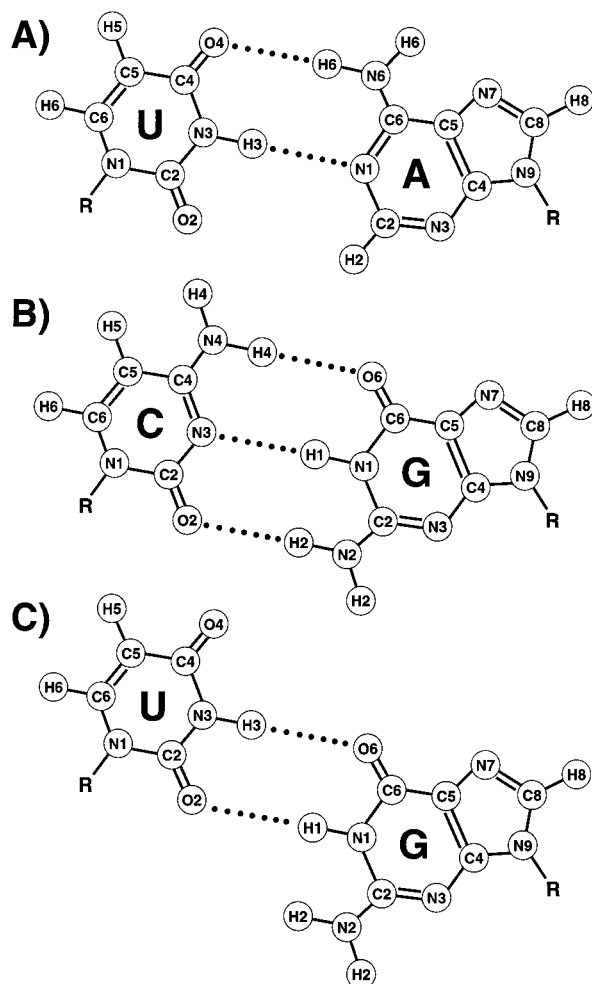


Figure 2. Hydrogen bond patterns and nomenclature for (A) U-A, (B) C-G, and (C) U-G base pairs.

time point c has decayed to $\exp(-4R_2T)[H3_\alpha N3_y \exp(-4\eta T) - H3_\beta N3_y \exp(4\eta T)]$. Therefore, the absolute amplitude of the $H3_\beta N3_y$ component at time point c is a factor $\exp(8\eta T)$ larger than the amplitude of the $H3_\alpha N3_y$ component. This factor is approximately 7–8 at 25 °C for the 69 nucleotide RNA domain used in this study.

Pervushin et al.²⁴ have shown that magnetization of the type $H3_\beta N3_y$ can be transferred into $H3_x N3_\beta$ magnetization by using the TROSY pulse sequence. Compared to a conventional reverse INEPT step where both α - and β -components of the ^{15}N doublet are refocused into $H3_x$ magnetization, this approach results in a factor of $1/(1 + \exp(-8\eta T))$ loss in the intensity of the $H3_x N3_\beta$ line as compared to the $H3_x$ line containing both nitrogen components. In the present situation, this loss is overcompensated by the increased T_2 of the $H3_x N3_\beta$ magnetization resulting from destructive interference between the dipolar and the proton CSA relaxation. This increase in imino proton T_2 is approximately 30% at 25 °C for the PSTVd T1 domain. The sequence of pulses between time points c and d is similar to the TROSY sequence resulting in detection of imino proton magnetization of the form $H3_x N3_\beta$ at point d . However, the inclusion of appropriate water flip-back pulses protects the magnetization of the imino protons against magnetization loss due to the fast exchange with the water.¹⁶ Additionally, the original phase cycling scheme for selection of the $H3_x N3_\beta$ component has been replaced by the selection gradients G_4 and G_7 . As the experiment correlates frequencies of imino ^1H –

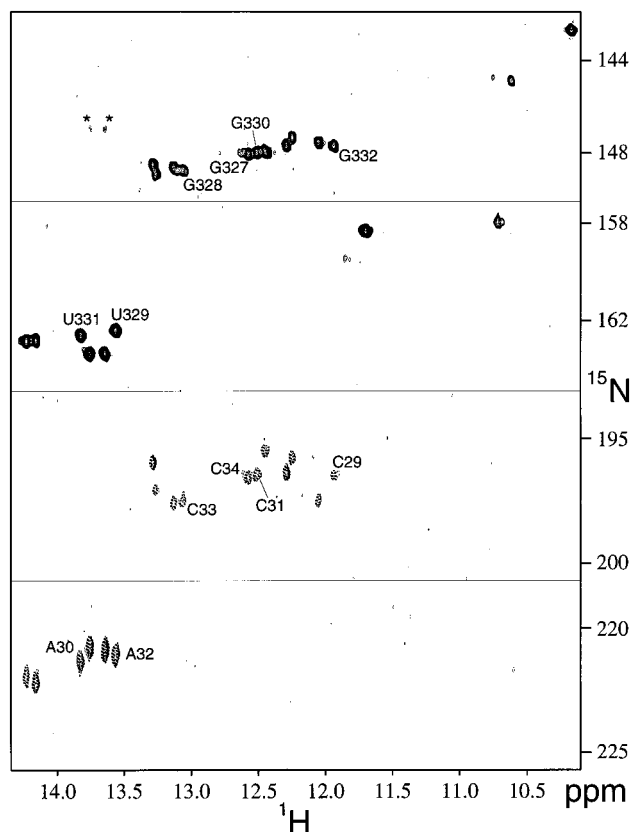


Figure 3. Quantitative J_{NN} HNN-COSY spectrum of the uniformly (>95%) $^{13}\text{C}/^{15}\text{N}$ -enriched 69-nucleotide T1 domain of the PSTVd RNA. Positive contours depict diagonal resonances, negative contours (dashed lines) correspond to cross-peaks resulting from scalar ^{15}N – ^{15}N magnetization transfer. Resonances are labeled with currently available assignment information. Two weak intranucleotide correlations between the N3 and N1 nuclei of uridine are marked with asterisks.

^{15}N resonances to the adjacent J -correlated ^{15}N nuclei, the pulse scheme is called quantitative J_{NN} HNN-COSY.

Figure 3 shows the results of a 12.3 h quantitative $^2J_{\text{NN}}$ HNN-COSY experiment for the T1 domain of PSTVd. A total of 6 correlations are observed between the uridine imino groups and ^{15}N resonances between 220 and 225 ppm, whereas 12 correlations are observed between the guanosine imino groups and ^{15}N resonances between 195 and 200 ppm. Additionally, two weak correlations are observed from the imino groups of uridine to ^{15}N resonances at approximately 147 ppm (Figure 3, asterisks). The latter two correlations were assigned to intraresidue two-bond transfers from the N3 to the N1 nucleus of uridine.

Initially the correlations to resonances below 195 ppm were highly unexpected and their assignment was unclear. Based on the chemical shifts of the cross-peaks, intraresidue J_{NN} correlations to N2, N3, N7, and N9 of guanosine or to N1 of uridine can be excluded.⁹ Besides such intraresidue correlations, the closest nitrogen nuclei for the imino nitrogens are the hydrogen bond acceptor ^{15}N nuclei on the opposing base for Watson–Crick base pairs. The observed chemical shift range of 195 to 200 ppm for the guanosine cross-peaks corresponds closely to the values reported for the $^{15}\text{N}3$ nucleus of cytidine.⁹ There are no other ^{15}N nuclei resonating near this frequency. In contrast, for the uridine cross-peaks between 220 and 225 ppm assignment is possible to either the $^{15}\text{N}3$ or $^{15}\text{N}1$ frequencies of adenosine, as the reported values for both nuclei are in close proximity to this chemical shift range.⁹ The chemical shift of both of these ^{15}N nuclei is strongly influenced by the

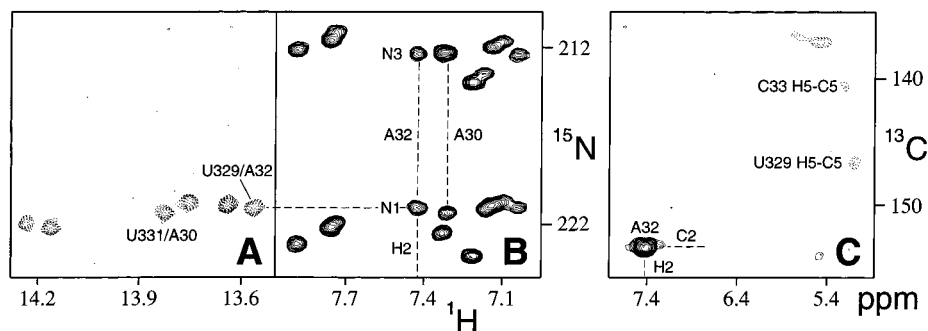


Figure 4. Establishment of cross hydrogen bond assignments for the U329-A32 base pair of the T1 domain of the PSTVd RNA. Resonances are labeled with currently available assignment information. (A) Region of the quantitative J_{NN} HNN-COSY spectrum depicting interstrand $^1\text{H}3$ – $^{15}\text{N}3(\text{U})$ to $^{15}\text{N}1(\text{A})$ correlations. (B) Region of the two-bond J_{HN} HSQC experiment correlating $^1\text{H}2$ frequencies of adenosine to the intrasidue $^{15}\text{N}1$ and $^{15}\text{N}3$ frequencies. (C) Cross section taken at the $^1\text{H}3$ frequency of U329 (13.56 ppm) from a ^{13}C -edited 3D NOESY spectrum recorded in H_2O . This cross section establishes the connectivity between $^1\text{H}3$ of U329 and the $^1\text{H}2$ – $^{13}\text{C}2$ frequency pair of the opposing A32.

protonation state of the base.^{9,25,26} Upon protonation, upfield shifts as large as 60–70 ppm have been observed for the N1 nucleus of adenosine.^{9,25} Despite this ambiguity in chemical shifts, the N3 nucleus of adenosine is separated by four chemical bonds (including the hydrogen bond) from the N3 nucleus of uridine, whereas the N1 nucleus of adenosine is separated by only one chemical bond and one hydrogen bond. Therefore, and because of the analogy to the G-C base pair, we conclude that the correlations between the N3 nuclei of uridine to resonances between 220 and 225 ppm must be interpreted as correlations to the hydrogen-bonded $^{15}\text{N}1$ nuclei of the opposing adenosine bases rather than to their $^{15}\text{N}3$ nuclei.

The assignments of the interresidue cross-peaks in the case of U-A base pairs are corroborated by two additional experiments: a three-dimensional ^{13}C -edited NOESY and a two-bond ^1H – ^{15}N -HSQC. Figure 4A shows the region of the U-A cross-peaks from the quantitative HNN-COSY experiment with the assignment of the U329-A32 correlation in the PSTVd T1 domain. The plane from the three-dimensional ^{13}C -edited NOESY (Figure 4C) taken at the frequency of the imino $^1\text{H}3$ proton of U329 shows a strong NOE correlation to the H2 proton of A32. This cross-peak establishes the assignment of the $^1\text{H}2$ – $^{13}\text{C}2$ frequencies of A32. The $^1\text{H}2$ frequency of A32 is correlated to the ^{15}N frequencies of N1 and N3 of A32 by the two-bond ^1H – ^{15}N -HSQC experiment (Figure 4B). The $^{15}\text{N}1$ frequency of A32 in this experiment is identical to the $^{15}\text{N}1$ frequency observed for the $^1\text{H}3(\text{U329})$ – $^{15}\text{N}1(\text{A32})$ cross-peak of the HNN-COSY experiment in Figure 4A. For the other five U-A cross-peaks of the HNN-COSY (Figure 4A), analogous connections are observed between the uridine $^1\text{H}3$ and adenosine $^{15}\text{N}1$ frequencies of the HNN-COSY, the adenosine $^1\text{H}2$ and $^{15}\text{N}1$ frequencies of the two-bond ^1H – ^{15}N -HSQC experiment (Figure 4B), and the uridine $^1\text{H}3$ and adenosine $^1\text{H}2$ correlations of the ^{13}C -edited NOESY (data not shown).

No interresidue correlations are observed in the HNN-COSY for imino groups with proton chemical shifts upfield of 11.8 ppm (Figure 3). This proton chemical shift range is usually indicative of non-Watson–Crick base pairs, such as G-U base pairs (Figure 2C). For these imino resonances, the lack of cross hydrogen bond ^{15}N – ^{15}N correlations is rationalized by the fact that most non-Watson–Crick base pairs contain hydrogen bonds from an imino hydrogen to an oxygen acceptor atom rather than to a nitrogen atom (Figure 2C).

The secondary structures which have been proposed for the

PSTVd T1 domain are of rodlike or bifurcated form.^{27–29} Both model types predict approximately 22 Watson–Crick base pairs (8 U-A and 14 G-C pairs) and 2–3 non-Watson–Crick base pairs. Considering the possible loss of some of the cross-peaks due to imino proton exchange with water, the observed 6 U-A and 12 G-C correlations in the HNN-COSY experiment are in reasonable agreement with this prediction.

To give further evidence that the magnetization transfer follows the expected behavior for a scalar coupling, the transfer time $2T$ in the HNN-COSY experiment was varied from 15 to 60 ms. Figure 5A shows cross-peak (I_c) and diagonal peak (I_d) intensities as a function of the transfer time for the $^1\text{H}3(\text{U})$, $^{15}\text{N}3(\text{U})$, and $^{15}\text{N}1(\text{A})$ nuclei of a UA base pair. A fit of these intensities according to $A\exp(-4T/T_2)\sin^2(2\pi JT)$ for cross-peaks and $A\exp(-4T/T_2)\cos^2(2\pi JT)$ for diagonal peaks yielded values for J of 6.78 Hz and for T_2 of 70.6 ms. This extracted J coupling is in very close agreement with the J coupling of 6.89 Hz derived from a single HNN-COSY experiment with a transfer time $2T$ of 30 ms (see below). Clearly, the fit reproduces the experimental points in a very satisfactory manner. Similarly, a plot of $\text{atan}([I_c/I_d]^{1/2})$ versus the transfer time T (Figure 5B) shows excellent agreement with the expected linear dependence.

Quantitative values for the observed $^2J_{NN}$ couplings can be determined from the ratio of cross-peak to diagonal peak intensities²¹ ($[I_c/I_d] = \tan^2(2\pi J_{NN}T)$) of a single HNN-COSY experiment. Due to the partial cancellation of dipolar and ^{15}N -CSA interactions, the line widths of the diagonal resonances in the HNN-COSY are considerably narrower than the line widths of the cross-peaks (Figure 3). Therefore, approximating the intensity ratios by peak amplitude ratios would introduce large errors. Instead, the ratio of diagonal and cross-peak intensities was determined as the amplitude ratio of the time domain oscillations for these resonances. These time domain amplitudes were derived from the data by using the time domain fitting routine *nlinLS* contained in the NMRPipe package.¹⁹ For the HNN-COSY experiment with a transfer time $2T = 30$ ms, values for cross hydrogen bond $^2J_{NN}$ couplings were determined as 6.7 ± 0.5 Hz ($n = 6$) for the observed U-A base pairs and as 6.3 ± 0.2 Hz ($n = 8$) for the well-resolved resonances of the G-C base pairs. The magnetization transfer in the HNN-COSY experiment is affected to some extent by the finite strength of

(27) Riesner, D.; Henco, K.; Rokohl, U.; Klotz, G.; Kleinschmidt, A. K.; Domdey, H.; Jank, P.; Gross, H. J.; Sanger, H. L. *J. Mol. Biol.* **1979**, *133*, 85–115.

(28) Steger, G.; Hofmann, H.; Fortsch, J.; Gross, H. J.; Randles, J. W.; Sanger, H. L.; Riesner, D. *J. Biomol. Struct. Dyn.* **1984**, *3*, 543–571.

(29) Gast, F.-U.; Kempe, D.; Spieker, R. L.; Sanger, H. L. *J. Mol. Biol.* **1996**, *262*, 652–670.

(25) Buchanan, G. W. *Tetrahedron* **1989**, *45*, 581–604.

(26) Wang, C.; Gao, H.; Gaffney, B. L.; Jones, R. A. *J. Am. Chem. Soc.* **1991**, *113*, 5486–5488.

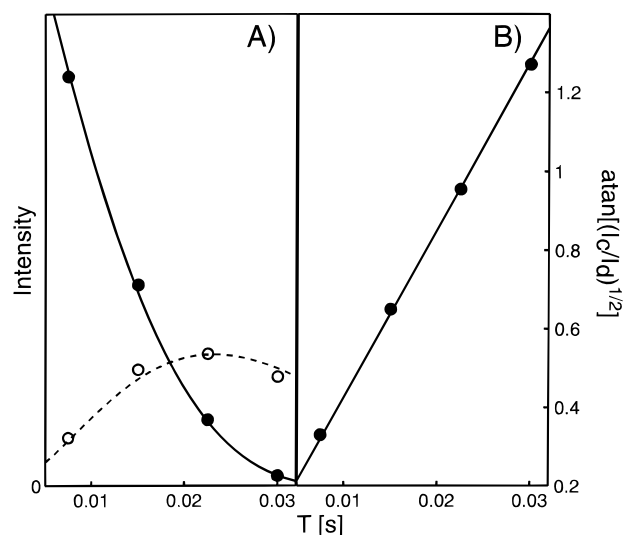


Figure 5. (A) Absolute values of cross-peak (I_c , open circles) and diagonal peak (I_d , filled circles) intensities observed in the HNN-COSY experiment as a function of the transfer time T . The intensities were derived for the correlation of the $^1\text{H3(U)}$, $^{15}\text{N3(U)}$, and $^{15}\text{N1(A)}$ nuclei of the U356-A343 or U356-A4 base pair (the assignment of A343 versus A4 is currently ambiguous). The continuous lines show the result of a simultaneous fit by the functions $A\exp(-4T/T_2)\sin^2(2\pi JT)$ for cross-peaks and $A\exp(-4T/T_2)\cos^2(2\pi JT)$ for diagonal peaks ($T_2 = 70.6$ ms, $J = 6.78$ Hz). (B) Plot of $\phi = \text{atan}([I_c/I_d]^{1/2})$ for experimental intensities (filled circles) shown in (A) versus the transfer time T . The continuous line corresponds to the theoretical dependence $\phi = 2\pi JT$ with the value of J derived from the fit in (A).

the ^{15}N rf field (5.9 kHz) as compared to the relative large frequency offsets (730–2300 Hz at 14.1 T , carrier at 185 ppm) of the $^{15}\text{N1}$ and $^{15}\text{N3}$ resonances. A numerical simulation shows that this results in an underestimation of the couplings by approximately 10–15% for U-A base pairs whereas G-C base pairs are affected to a lesser extent. Even without this correction, the $^2J_{\text{NN}}$ couplings derived for U-A base pairs are slightly larger than the values for G-C base pairs. It is remarkable that the stronger coupling for U-A coincides with a shorter N-N distance [2.82 Å (U-A) vs 2.95 Å (G-C)] observed in crystal structures.² In agreement with previous results,³⁰ the intensities of the two observed intrasidue N3–N1 correlations in uridine correspond to values of 2.1 ± 0.3 Hz for these $^2J_{\text{N3N1}}$ couplings (see Figure 3).

For the T1 domain of PSTVd, observed T_2 values for ^{15}N diagonal resonances in the HNN-COSY experiment range between 50 and 70 ms. It is therefore expected that a direct splitting of such resonances due to the 7 Hz trans hydrogen-bond scalar coupling can only be observed with rather low sensitivity. Such in-phase splittings are, however, observed in the ^{15}N cross sections of a 12 h two-dimensional ^1H – ^{15}N TROSY²⁴ experiment (data not shown).

At present, the exact mechanism of polarization transfer via the hydrogen bond is unclear. In principle, cross correlation

(30) Büchner, P.; Maurer, W.; Rüterjans, H. *J. Magn. Reson.* **1978**, *29*, 45–63.

between dipolar/dipolar or dipolar/CSA Hamiltonians could lead to magnetization transfer^{31–34} between the ^{15}N nuclei adjacent to the hydrogen bond. These effects are, however, considerably smaller than the observed transfer rates of approximately 7 Hz. For a three-spin system consisting of the $^1\text{H3}$ and $^{15}\text{N3}$ nuclei of uridine and the $^{15}\text{N1}$ nucleus of the opposing adenosine, the possible values for the dipolar and CSA interaction energies and the Larmor frequencies lead to cross correlated relaxation rates between the $^{15}\text{N3(U)}$ and the $^{15}\text{N1(A)}$ nuclei that are below 1 Hz for correlation times ranging from 5 to 40 ns. (A detailed numerical calculation is given in the Supporting Information.) The principal reason for this finding is that these cross correlation effects must involve the rather small dipolar couplings between the $^{15}\text{N3(U)}$ and $^{15}\text{N1(A)}$ nuclei or the $^1\text{H3(U)}$ and $^{15}\text{N1(A)}$ nuclei. It is therefore concluded that such “dynamic” J couplings cannot explain the observed phenomena and that a conventional polarization of the electron cloud in the hydrogen bond is the likely explanation for the observed trans hydrogen-bond scalar interactions. A related interaction mediated by sulfur electronic orbitals has been observed between amide protons and ^{113}Cd in the iron–sulfur protein rubredoxin.³⁵

It should be noted that the observed couplings can compromise T_2 measurements for imino ^{15}N nuclei if the interstrand $^2J_{\text{NN}}$ couplings are not properly decoupled. On the basis of the almost identical chemical structure, we expect similar cross hydrogen-bond $^2J_{\text{NN}}$ couplings for Watson–Crick base pairs in ^{15}N -enriched DNA. The HNN-COSY experiment is rather sensitive even for larger oligonucleotides and should provide valuable interstrand assignment information.

Acknowledgment. We thank Bernd Esters for expert help during sample preparation, Detlev Riesner and Gerhard Steger for stimulating discussions, and Georg Büldt for continuous support. We also thank the referees for their valuable suggestions. A.J.D. acknowledges funding by the Australian National Health and Medical Research Council C.J. Martin Fellowship (Regkey 987074). This work was supported by DFG Grant No. GR1683/1-1.

Supporting Information Available: Calculation of dipolar/dipolar or dipolar/CSA cross correlation effects which could lead to J -like ^{15}N – ^{15}N magnetization transfer in a ^{15}N – ^1H – ^{15}N spin system (4 pages, print/PDF). See any current masthead page for ordering information and Web access instructions.

JA981513X

(31) Werbelow, L. G. In *Encyclopedia of Nuclear Magnetic Resonance*; Grant, D. M., Harris, R. K., Editors-in-Chief; Wiley: London, 1996; Vol. 6, pp 4072–4078.

(32) Tjandra, N.; Grzesiek, S.; Bax, A. *J. Am. Chem. Soc.* **1996**, *118*, 6264–6272.

(33) Theis, K.; Dingley, A. J.; Hoffmann, A.; Omichinski, J. G.; Grzesiek, S. *J. Biomol. NMR* **1997**, *10*, 403–408.

(34) Wimperis, S.; Bodenhausen, G. *Mol. Phys.* **1989**, *66*, 897–919.

(35) Blake, P. R.; Park, J. B.; Adams, M. W. W.; Summers, M. F. *J. Am. Chem. Soc.* **1992**, *114*, 4931–4933.